nzsee
NEW ZEALAND SOCIETY FOR EARTHQUAKE ENGINEERING

# Earthquake strengthening clay brick masonry parapets – proof-tested solutions

*Marta Giaretton, Dmytro Dizhur*

DIZHUR Consulting, Auckland, New Zealand

*Jason Ingham*

University of Auckland, Auckland, New Zealand

## ABSTRACT

Unrestrained unreinforced clay brick masonry (URM) parapets are found atop of a large number of vintage URM buildings. Parapets are typically cantilevered wall structural elements that form decorative and ornamental features of the building facades or in case of building side parapets, form a fire barrier. Due to the elevated location and the extent of the parapets above the main street frontage and main building entrances, parapets are considered the most vulnerable element that is prone to out-of-plane collapse during an earthquake.

Numerous observations following recent earthquakes in New Zealand and internationally suggest that URM parapets that were previously secured performed below expectations. Subsequently, a shake-table experimental program was implemented to investigate the seismic performance of various types of parapet restraints. The objective of the study was to provide building owners and practicing engineers with industry-accepted proof-tested retrofit solutions for securing of URM parapets, including the use of steel brace, timber brace and post-tensioning. Results and observations from the experimental study are presented herein.

## 1 INTRODUCTION

Unreinforced masonry (URM) parapets are free-standing non-structural components that pose a significant falling hazard and in past earthquakes have caused numerous injuries and required costly repairs [1–3]. To mitigate this hazard, some communities have adopted ordinances that require URM parapets to be secured or

removed [4–6]. Nevertheless, the absence of detailed recommendations resulted in the implementation of a mixture of seismic improvement techniques, which leads to a wide range of seismic performance levels for the secured parapets as described in [1]. Between the causes of failure of retrofitted parapets there was the presence of poorly detailed connections leading to corrosion, substandard installation of masonry anchors, short embedment of masonry anchors, and poorly designed load paths of the retrofit were identified as some of the causes of out-of-plane collapse of braced parapets, [1, 3].

Previous studies on parapets focused mainly in the earthquake performance of as-built URM parapets developing fragility curves [7, 8], analysing the free-rocking behaviour [9], and providing an assessment procedure to evaluate the dynamic out-of-plane stability of cracked URM parapets located in multi-storey URM buildings [10–12]. [13] performed shake-table tests of two full-scale one-storey clay brick masonry walls with URM parapets above and a flexible diaphragms. One of the tests was undertaken after retrofitting the parapet with steel braces and wall-to-floor diaphragm connections. Although previous studies have provided insight into the out-of-plane response of URM parapets, there is a lack of experimental results that consider the variation of parameters such as parapet height, mortar strength and retrofit system, and investigate dynamic behaviour after cracking. Information acquired during a previous pilot study [1] was used to identify common construction details and material properties with the aim of simulating a central portion of the façade of a common single- or multi-storey URM building. A comprehensive shake-table campaign was undertaken on 13 full-scale solid clay brick URM parapets, nine of those where then retrofitted and subjected again to dynamic loading. The retrofit techniques investigated were the installation of braces with and without diaphragm anchors, the use of post-tensioning, and the combination of braces and vertical strong-backs, as shown in **Figure 1**.

(a) Steel brace and diaphragm anchors

(b) Timber brace and diaphragm anchors

(c) Timber brace and vertical strong-backs

(d) Post-tensioning

*Figure 1. Retrofit systems applied and tested.*

## 2 EXPERIMENTAL PROGRAMME

Thirteen full-scale solid clay brick masonry parapets were tested in an as-built condition to evaluate their earthquake performance and to serve as a control to quantify the level of performance improvement of nine parapets retrofitted with selected techniques. The tested as-built URM parapets ranged between 720 mm and 1605 mm in height and were constructed using different mortar mixes to investigate the influence of mortar conditions on the seismic capacity of parapets. The adopted width of 1200 mm was related to the maximum dimensions that could be accommodated on the shake-table. Brick dimensions were of standard size (230L × 110W × 75H mm) for heritage masonry construction and the brick compressive strength was 26.4 MPa. Three different mortar mixes were used, being 1:2:9 (referred to as mix 'A', with the highest compressive strength, 3.2 MPa), 1:3:12 (noted as mix 'B', 2.2 MPa), and 0:1:3 (referred to as mix 'C', with the lowest compressive strength, 0.5 MPa) (cement:lime:sand) by volume, to simulate the common field conditions of vintage mortar with variable strength ranging from moderately strong (A) to severely deteriorated due to weathering (C). The masonry compressive strength was respectively 12.8 MPa, 10.7 MPa, and 7.4 MPa. **Table 1** shows the summary test matrix.

*Table 1. Test matrix*

| **Parapet ID (as-built)** | **Parapet H (mm)** | **Parapet T (mm)** | **Wall T (mm)** | **Mortar mix *** | **Retrofit type** | **Parapet ID (retrofitted)** |
|---|---|---|---|---|---|---|
| P1-C(1605) | 1605 (19) | 230 | 350 | 0:1:3 (C) | Timber brace | P1-C(1605)TB |
| P2-A(1180) | 1180 (14) | 230 | 350 | 1:2:9 (A) | Steel brace | P2-A(1180)SB |
| - | 1180 (14) | 230 | 350 | 1:2:9 (A) | Timber brace | P2-A(1180)TB |
| - | 1180 (14) | 230 | 350 | 1:2:9 (A) | Post-tensioning | P2-A(1180)PT |
| P3-A(1180) | 1180 (14) | 230 | 350 | 1:2:9 (A) | n/a | - |
| P4-B(1180)** | 1180 (14) | 230 | 230 | 1:3:12 (B) | Timber brace | P4-B(1180)TB ** |
| P5-B(1180) | 1180 (14) | 230 | 350 | 1:3:12 (B) | Steel brace | P5-B(1180)SB |
| P6-B(1180)45** | 1180 (14) | 230 | 230 | 1:3:12 (B) | Timber brace and vertical strong-backs | P6-B(1180)TBS ** |
| P7-C(1180)** | 1180 (14) | 230 | 230 | 0:1:3 (C) | Timber brace and vertical strong-backs | P7-C(1180)TBS ** |
| P8-C(1095) | 1095 (13) | 230 | 350 | 0:1:3 (C) | n/a | - |
| P9-B(1060) | 1060 (12) | 230 | 230 | 1:3:12 (B) | n/a | - |
| P10-C(975) | 975 (11) | 230 | 230 | 0:1:3 (C) | n/a | - |
| P11-B(805) | 805 (9) | 230 | 230 | 1:3:12 (B) | n/a | - |
| P12-A(720) | 720 (8) | 230 | 230 | 1:2:9 (A) | n/a | - |
| P13-C(720) | 720 (8) | 230 | 230 | 0:1:3 (C) | n/a | - |
| - | 1180 (14) | 230 | 350 | 0:1:3 (C) | Timber brace | P14-C(1180)TB |

(#) – number of brick courses; * cement:lime:sand; ** Phase-1 parapets, with P6 oriented at 45° to the direction of the shake table motion; Note: All parapets were 1200 mm wide

Parapets P1 to P3, P5, and P8 were constructed with an increase in the cross-section of the wall below which was three brick courses high and three leaves thick, providing a ledge on which the timber roof members were laid, see **Figure 2a,c**. For the remaining parapets, the cross-section was constant throughout the parapet height, representing a short section of wall three brick courses high and two leaves thick, see **Figure 2a,b**.

The experimental program was performed in two phases.
Phase 1 was undertaken using a 300 kN-capacity single-axis shake-table with dimensions of 3600 × 2400 mm capable of reproducing earthquake motions and involved three parapets, being P4-B(1180), P6-B(1180), and P7-C(1180). The ground motion recorded during the 22 February 2011 Christchurch earthquake (New Zealand), [14], was selected in order to compare the findings with data collected during post-earthquake reconnaissance [1].
The availability of the large shake-table was limited so the research team also used a purpose-built shake-table capable of applying unidirectional harmonic excitations to test multiple parapets with different parameters within a reasonable timeframe (Phase 2), see **Table 1**. The results collected during Phase 2 were then validated against the results attained during Phase 1.

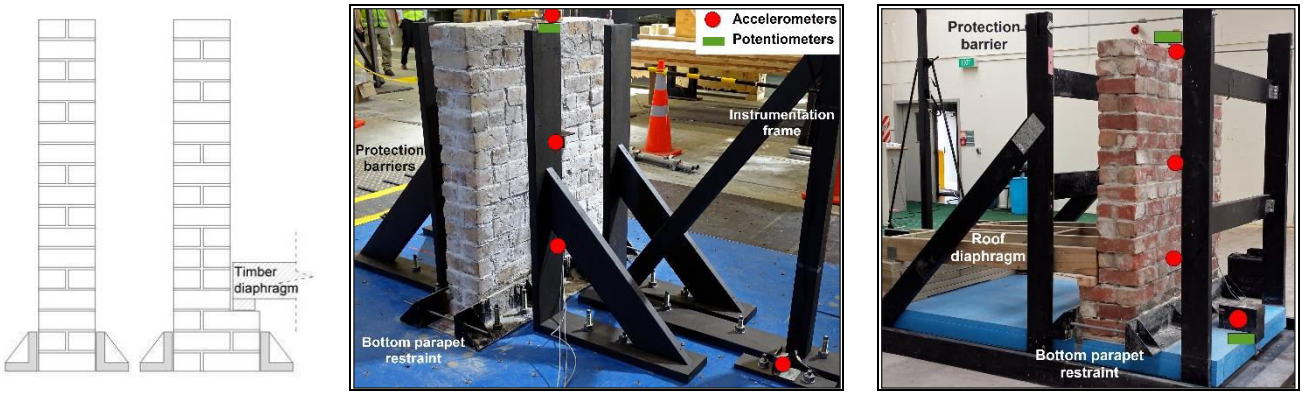


(a) Parapets cross-section (b) Phase-1 set-up (c) Phase-2 set-up

*Figure 2. Typical parapets set-up*

## 2.1 Test set-up

The samples were fixed at the base using two stiff steel base angles in order to replicate the field condition of a free-standing URM parapet positioned above a load-bearing URM wall. Protection barriers were designed and fixed onto the shake-table on both sides at a distance of approximately 210-220 mm away from the sample to prevent full collapse and protect the testing instrumentation. Three accelerometers were installed on one side of each parapet at the bottom, middle and top as shown in **Figure 2b,c**. An additional accelerometer was fixed onto the shake-table in order to record the effective horizontal acceleration produced. Two string potentiometers were attached at the top of the parapet and onto the shake-table to measure the differential displacement of the sample, see **Figure 2b,c**. The string potentiometers were mounted on a purpose-built instrumentation frame independent of the sample and the protection barriers.

## 3 CRACK-PATTERN AND FAILURE MODE

The tested as-built URM parapets typically failed along the mortar joints at the parapet base, see **Figure 3a,** as observed in a large number of as-built parapets damaged during the 2010/2011 Christchurch earthquakes [1]. After cracking, all tested as-built URM parapets exhibited rigid-body rocking behaviour that led to instability and eventual collapse. The use of a weaker mortar (mix C) expedited the dissipation of seismic energy, leading to the formation of multiple cracks at the bottom of the parapets.

The installation of the retrofit systems in cracked parapets significantly improve the observed performance and parapets built with strong mortar (mix A) did not sustain additional damage even at high level of shaking intensity. The number and size of cracks that developed in retrofitted parapets constructed with weak mortar increased with increasing motion amplitude, with Group C parapets exhibiting the heaviest damage pattern. Inward sliding failure (see **Figure 3b**) occurred at the existing crack plane at the base of P4-B(1180)TB and was attributed to the 20% increase in clear height between the base and top brace connection, recognising that P4-B(1180)TB had a brace fixed directly to the shake-table instead of the roof-diaphragm as P2-A(1180)TB. Other causes of failure include the pounding effect of the timber roof-diaphragm which occurred at high magnitudes of table acceleration in braced parapet P5-B(1180)SB retrofitted without installing the diaphragm anchors, as shown in **Figure 3c**. Finally, the development length of the steel post-tensioning bars below the diaphragm level was insufficient to prevent the initiation of parapet rocking and lead to collapse, see **Figure 3d**. **Figure 3e** shows the deterioration of the entire parapet surface and subsequent collapse of the masonry portion above the horizontal spreader strip in P7-C(1180)TBS retrofitted using the combined installation of brace, vertical strong-backs, and masonry anchors.

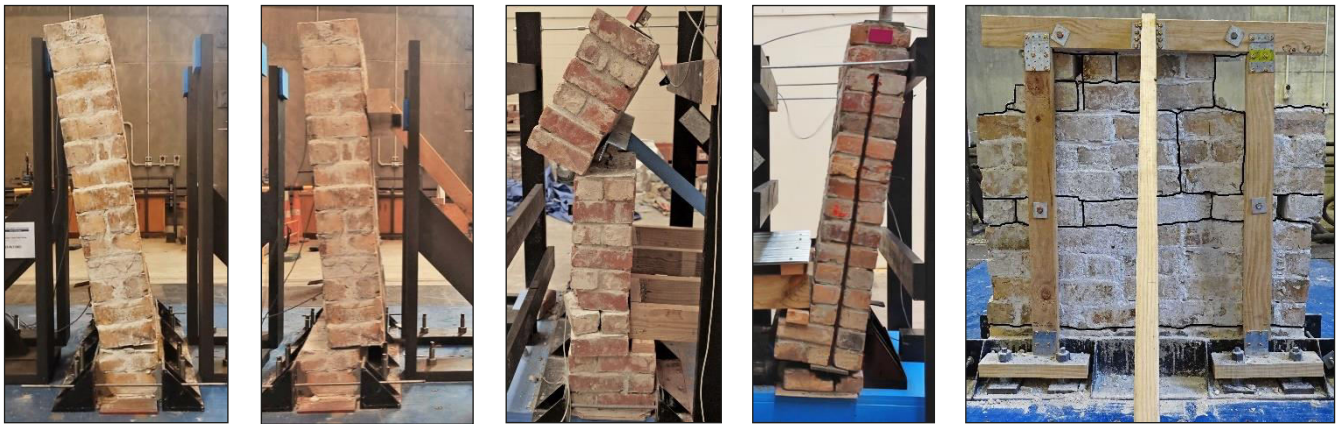

(a) P4-B(1180) (b) P4-B(1180)TB (c) P5-B(1180)SB (d) P2-A(1180)PT (e) P7-C(1180)TBS

*Figure 3. Observed failure modes*

# 4 PARAPET RESPONSE

## 4.1 As-built parapets

For as-built parapets it was observed that the formation of cracking led to rapid wall instability, so the test was stopped once cracking initiated as this damage state was deemed to correspond to a near collapse condition. Each test was then repeated in order to evaluate the peak table acceleration required to initiate rocking of the cracked as-built parapet. **Figure 4** shows the peak table acceleration values achieved for each parapet at the two different stages of wall behaviour, and also the maximum displacement recorded at parapet instability during the first test. Good correlation was found in terms of behaviour and peak acceleration when comparing the values among the tested parapets using the 22 February 2011 Christchurch earthquake motion (Phase 1) and parapets tested using harmonic motion (Phase 2). **Figure 5** shows the peak acceleration distribution profile along the parapet height, with the data being normalised with respect to table acceleration in order to simplify the comparison.

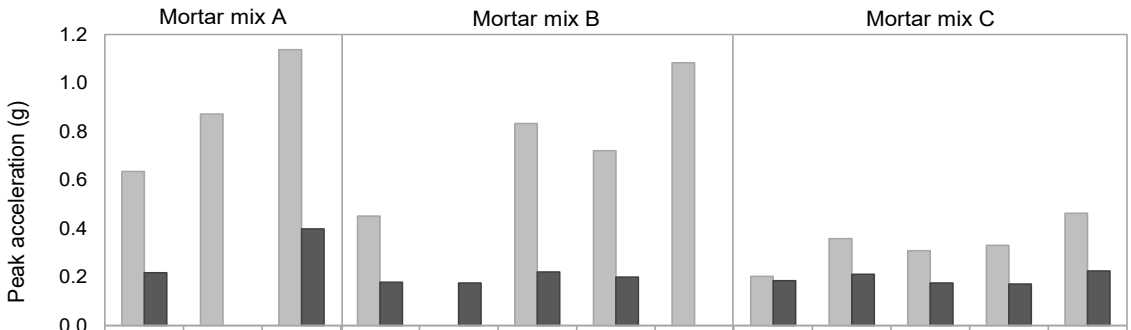


| | P2-A(1180) | P3-A(1180) | P12-A(720) | P4-B(1180) | P5-B(1180) | P6-B(1180) 45 | P9-B(1060) | P11-B(805) | P1-C(1605) | P7-C(1180) | P8-C(1095) | P10-C(975) | P13-C(720) |
|---|---|---|---|---|---|---|---|---|---|---|---|---|---|
| Cracking (g) | 0.64 | 0.87 | 1.14 | 0.45 | n/a | 0.83 | 0.72 | 1.08 | 0.20 | 0.36 | 0.31 | 0.33 | 0.46 |
| Rocking (g) | 0.22 | n/a | 0.40 | 0.18 | 0.18 | 0.22 | 0.20 | n/a | 0.19 | 0.21 | 0.18 | 0.17 | 0.23 |
| Displacement (mm) | 67.31 | 55.21 | 93.01 | 121.17 | n/a | 153.33 | 123.98 | 88.13 | 34.07 | 99.50 | 105.67 | 165.45 | 202.50 |

*Figure 4. As-built parapets. The peak table acceleration achieved is shown in light grey for initial cracking and dark grey for initiation of rocking. The maximum displacement was recorded prior instability during the first test. Data are clustered per type of mortar mix*

The recorded peak table acceleration at cracking was influenced by mortar strength. In P2-A(1180), cracks appeared at 0.64g while for parapets P4-B(1180) and P7-C(1180), cracking appeared at 0.45g and 0.36g, revealing a reduction of peak table acceleration of 29% and 44%, respectively. Similar trends were observed in shorter parapets. The initiation of cracking was inversely proportional to the height of the parapet, particularly for mortar mix A and B, where the peak table acceleration achieved for short parapets were 1.8 times (1.14g, P12-A(720)) and 2.4 times (1.08g, P11-B(805)) higher, respectively, than the peak table accelerations reached for a parapet with a height of 1180 mm (0.64g and 0.45g for mortar mix A and B, respectively). In addition, shorter parapets exhibited a higher number of stable rocking oscillations before collapse. This relationship was less evident for parapets constructed with mortar mix C, where the peak table

acceleration reached by parapet P13-C(720) was 1.3 times (0.46g) higher than that of parapet P7-C(1180) (0.36g).

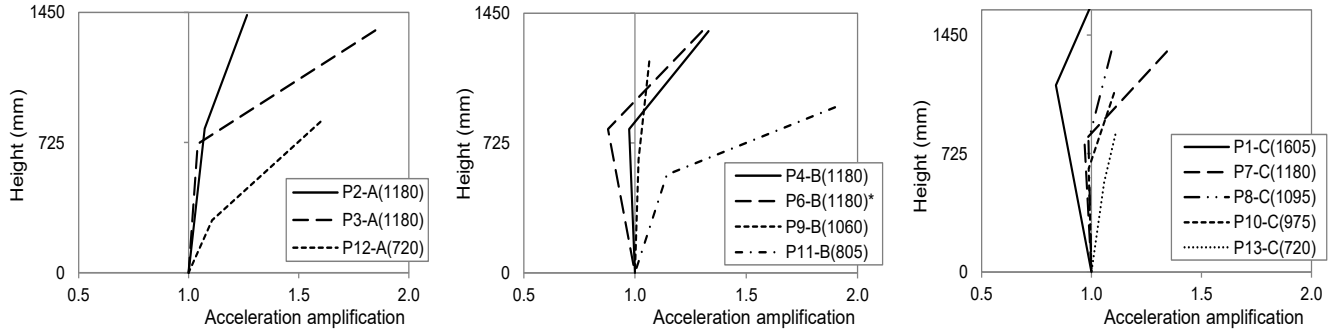


(a) Mortar mix A (b) Mortar mix B (c) Mortar mix C

*Figure 5. As-built parapets. Acceleration profiles at cracking. * tested at 45 degrees in relation to the direction of shake-table motion*

High acceleration of up to 1.3 to 1.9 times the peak table acceleration at cracking was recorded at the top of parapet groups A and B while at mid-height, acceleration was similar to the peak table acceleration (see **Figure 5a,b**). In parapet group C, top and mid-height acceleration was significantly reduced, likely due to the damping effect caused by the weaker mortar. At the top, measured acceleration was up to 1.3 times the peak table acceleration while at mid-height, it was 0.8 to 1.1 times the peak table acceleration (see **Figure 5c**).

Comparing the results obtained for parapet P4-B(1180), which was oriented normal to the direction of earthquake loading and P6-B(1180), which was positioned at 45° with respect to the axis of the shake-table motion, table acceleration 84% (0.83g) higher was required to induce cracking in the latter, corresponding to normal acceleration at the parapet base of 0.58g when accounting for the cos(45º) orientation of the table excitation. During post-crack testing, P6-B(1180) exhibited small oscillations during the test performed with 20% of input motion, and clear rocking behaviour was observed during the following load increment at 30% of input motion. Therefore, initial rocking is assumed to occur at a peak table acceleration value between the two tested amplitudes of input motion (0.22g and 0.38g, respectively) with rocking assumed to initiate at 0.30g. The corresponding value at the base of the parapet when accounting for the cos(45º) orientation of the table excitation was 0.21g, which is in accordance with theoretical calculations. For all other parapets that were tested in a post-crack condition, rocking commenced for table acceleration between 0.17g and 0.23g. In contrast to the response of the parapets oriented normal to the shake-table axis, where out-of-plane collapse occurred immediately after the initiation of rocking, better performance with stable rocking behaviour for table acceleration of up to 0.75g was observed in diagonally oriented parapets. This can be attributed to the influence of the substantial contribution of in-plane acceleration components to the restoring moment. This experimental finding is supported by the post-earthquake observation that parapets oriented orthogonally in the direction of earthquake loading are more vulnerable than parapets oriented diagonally.

The theoretical acceleration to induce as-built parapet rocking was calculated using simple static equations as suggested in Lam et al [9]. Dictated by the parapet h/t ratio, theoretical base acceleration was evaluated for parapet heights of 200 mm to 2000 mm and was consistent with test results, as shown in **Figure 6**. Lower theoretical acceleration (0.14g, 20% less than the experimentally measured value) was calculated for the tallest tested parapet, P1-C(1605), while for the shortest tested parapets, the experimental table acceleration required to cause rocking was 20% higher and 40% lower than the theoretical value (0.32g) for P12-A(720) and P13-C(720), respectively. **Figure 6** reports the estimated PGA curves for parapets located above single- or multi-storey buildings, which were calculated using the empirical equations provided in [15], Eq. (1). The estimated PGA curves were calculated using the floor height coefficient ($C_{Hi}$), Eq. (1) [15], with the typical building height at the roof line being considered: (i) 3000 to 3600 mm for a single-storey building; (ii) 5800 to 6600 mm for a two-storey building; and (iii) 8600 to 9600 mm for a three-storey building.

$$C_{Hi} = \left(1 + \frac{h_i}{6}\right) \quad \textbf{for all } h_i < 12 \text{ m where } h_i \textbf{ is the building height at the roof line} \qquad \text{ma}$$

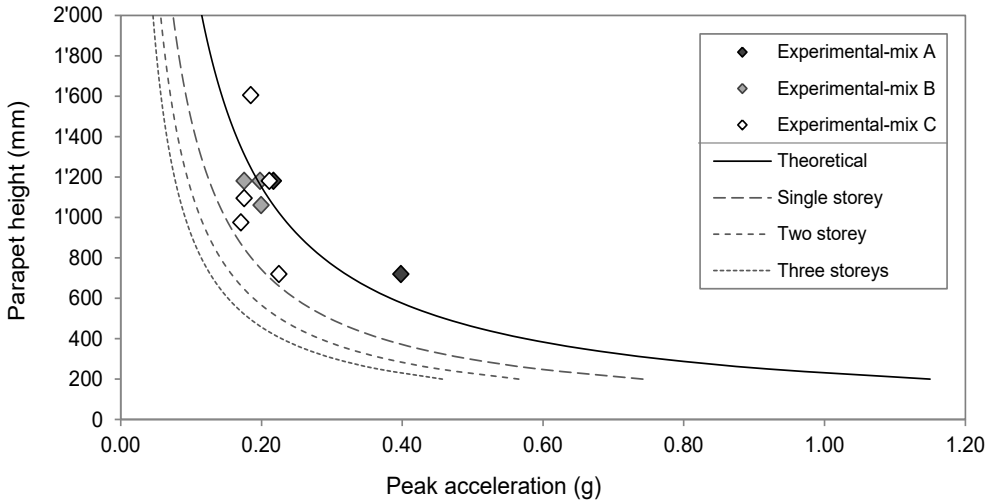


***Figure 6.*** *Theoretical and experimental parapet base acceleration required to induce rocking and corresponding estimated PGA for parapets located in single- and multi-storey buildings*

## 4.2 Retrofitted parapets

In **Figure 4** is evident that the acceleration necessary to cause cracking was distinctly greater than the acceleration required to generate rocking behaviour of the cracked parapet and thus a conservative estimate of the loads necessary to generate parapet cracking should be used when designing lateral parapet restraints. **Figure 7** compares the results of retrofitted parapets with rocking values recorded in as-built parapets P2-A(1180), P4-B(1180), and P7-C(1180).

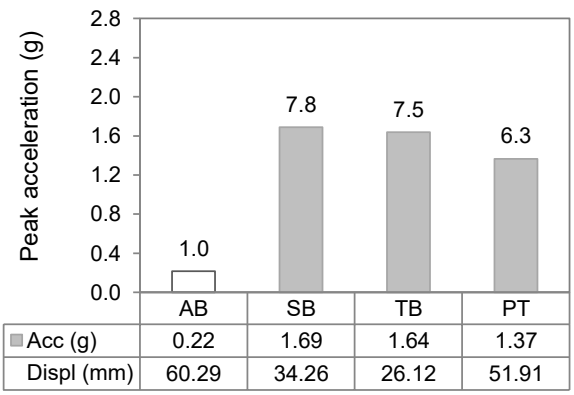


(a) As-built parapet P2-A(1180) and the corresponding retrofitted parapets

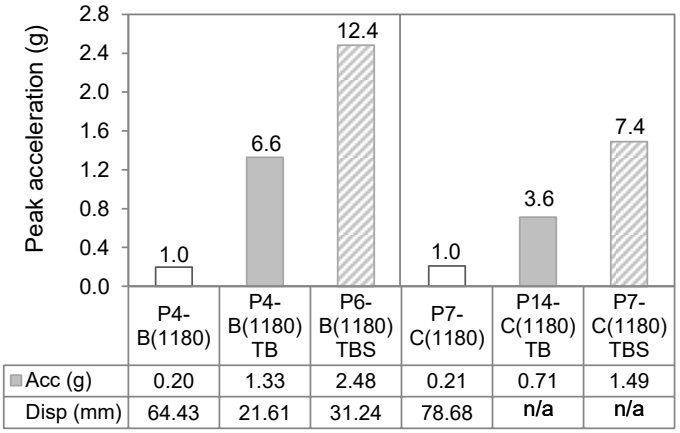


(b) Timber braced vs timber braced and vertical strong-back parapets

*Figure 7. Comparison of peak table acceleration values. Values at the top of each column indicate ratio of improvement relative to the as-built condition*

Parapets retrofitted with either a steel brace or a timber brace had similar performance, with the required table acceleration approximately eight times the value required for as-built parapets in the post-cracked condition (see **Figure 7a**). The steel-braced parapets, P2-A(1180)SB and P5-B(1180)SB, reached a peak table acceleration of approximately 1.69g, with the mid-height and top acceleration 1.2 and 1.7 times higher than the table acceleration, respectively. The maximum displacement recorded at the parapet top was 34 mm for P2-A(1180)SB and 50 mm for P5-B(1180)SB. Following the test for parapet P2-A(1180)SB with a steel brace, the bracing system was modified by swapping the steel brace for a timber brace (P2-A(1180)TB). The test was stopped at 1.64g with no observation of any further damage and a maximum top displacement of 26 mm. P4-B(1180)TB reached a 20% lower peak table acceleration (1.33g) compared to P2-A(1180)TB, which can be attributed to premature sliding failure due to the extent of clear height between the base and top brace connection and a maximum top displacement of 22 mm. P1-C(1605)TB was the tallest parapet to be tested and reached a peak table acceleration of 0.80g, with the mid-height and top accelerations 1.3 and 2.0 times greater than the peak table acceleration, respectively, and a maximum top displacement of 19 mm. The lowest peak table acceleration of 0.71g was achieved by P14-C(1180)TB. This result can be attributed to premature failure related to inappropriate positioning of the masonry anchors and the extensive formation of cracks.

The lowest level of peak table acceleration of 1.37g was recorded for the post-tensioned parapet P2-A(1180)PT, which can be attributed to the insufficient development length that failed to adequately engage the masonry wall below the parapet. The acceleration value at failure was six times that required for the as-built parapet and 20% lower than for the steel-braced parapet as shown in **Figure 7a**. The maximum near-collapse top displacement for P2-A(1180)PT was recorded at 50 mm. This corresponds to the maximum tension force recorded in the post-tensioning steel bar of 18.8 kN, which includes the applied pre-tensioning load of 13.0 kN. The installation of vertical strong-backs resulted in the highest level of recorded table

acceleration of 2.48g for P6-B(1180)TBS and 1.49g for P7-C(1180)TBS, being twice the value of that reached for parapets with the timber-brace only (see **Figure 7b**).

*Table 2.Summary of findings from retrofitted parapet tests*

| Parapet ID | Peak table acceleration (g) | Max top displacement (mm) | Failure mode |
|---|---|---|---|
| **Steel brace** | | | |
| P2-A(1180)SB | 1.69 | 34.3 | No damage ** |
| P5-B(1180)SB | 1.66 | 49.9 | Extensive cracks at roof level |
| P5-B(1180)SB * | 1.77 | 112.2 | Pounding of the roof-diaphragm |
| **Timber brace** | | | |
| P1-C(1605)TB | 0.80 | 19.4 | Masonry collapse above retrofit |
| P2-A(1180)TB | 1.64 | 26.1 | No damage ** |
| P4-B(1180)TB | 1.33 | 21.3 | Base shear sliding |
| P14-C(1180)TB | 0.71 | n/a | Masonry collapse above retrofit |
| **Timber brace and vertical strong-backs** | | | |
| P6-B(1180)TBS | 2.48 | 31.2 | Base shear sliding |
| P7-C(1180)TBS | 1.49 | n/a | Extensive cracks and masonry collapse above retrofit |
| **Post-tensioning** | | | |
| P2-A(1180)PT | 1.37 | 51.9 | Rocking at the base |

* Tested without diaphragm anchors; ** Maximum load generated by Phase 2 shake-table

Comparing these results with those for as-built parapets, seismic capacity in terms of acceleration improved by more than 12 and seven times for parapets built with mortar mixes B and C, respectively. The mid-height and top accelerations were 1.2 and 1.9 times greater than the table acceleration, respectively. The maximum top displacement recorded for P6-B(1180)TBS was 31 mm. For P7-C(1180)TBS, the string potentiometer was removed to avoid damage in case of collapse of portions of the masonry. **Table 2** shows a summary of the presented findings comparing the observed performance for each type of investigated retrofit technique. Using the floor height coefficient ($C_{Hi}$) calculated in accordance with [15], the effective PGA to cause failure of the retrofitted parapets was estimated in relation to the number of floors, as shown in **Figure 8**.

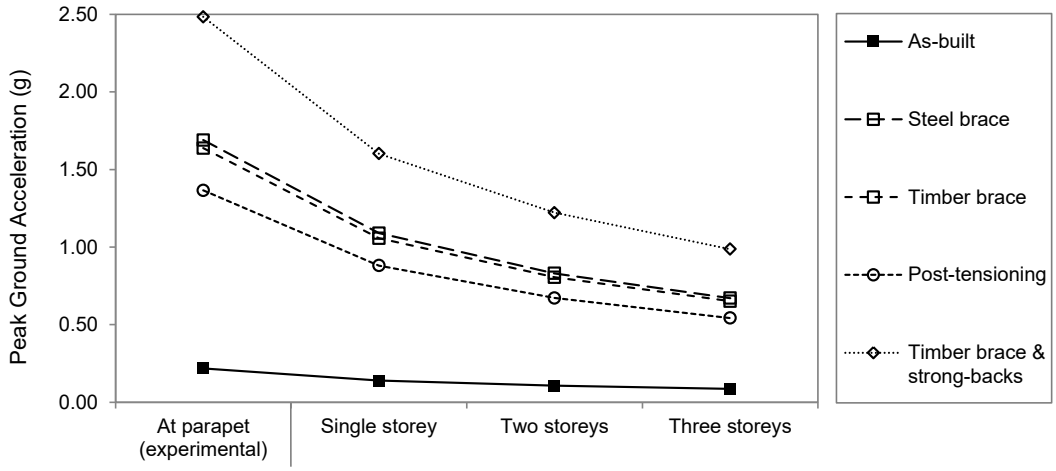


*Figure 8. Estimation of the effective PGA to cause parapet failure for a single-, two-, or three-storey URM building. Data presented refer to P2-A(1180) in as-built and retrofitted conditions while TBS refers to P6-B(1180)TBS*

## 5 CONCLUSIONS

The dynamic behaviour of 13 full-scale solid clay brick URM parapets was investigated by considering different configurations of parapet height and mortar mix. Nine of those parapets were then retrofitted and re-tested. The main findings of the research described herein are summarised below:

- The peak table acceleration that caused cracking is inversely proportional to the height of the parapet and directly proportional to the mortar strength. At the top of the parapets, the peak table acceleration was amplified up to 1.9 times, with lower values recorded in parapet group C due to the damping effect of the weak mortar.
- The PGA required to initiate cracking in an 1180 mm high parapet (mortar mix A) is estimated to be 0.41g, 0.32g, or 0.32g for single-, two-, and three-storey buildings, respectively.
- Rocking behaviour was initiated in a post-crack condition between 0.17g and 0.30g. Predicted capacities calculated using the simple static equilibrium approach were found to be accurate, suggesting that basic equations should be used to assess parapets' expected performance.
- The acceleration required to cause cracking is much greater than the acceleration required to cause rocking. Considering that many URM parapets typically present severely deteriorated mortar and pre-existing cracking, designs for securing parapets should be based on conservative estimates of the loads necessary to generate cracking.
- It was confirmed that parapets oriented normal to the earthquake loading direction are more vulnerable than diagonally oriented parapets. Table acceleration that is 84% higher was required to induce cracking of parapets positioned at 45° with respect to table motion. Rocking commenced at 0.30g, and parapets exhibited stable oscillation up to 0.75g instead of sudden collapse, as occurred with normally oriented parapets. A trigonometric relationship was observed between table motion and the acceleration recorded for the diagonally oriented parapets.

**Steel- and timber-braced parapets.** Braced parapets improved the seismic capacity by eight times the near-collapse magnitude of as-built parapets in their post-cracked condition. If durability measures are addressed, timber bracing can be considered a cost-effective securing alternative. The lack of connection (anchors) between the roof-diaphragm and masonry led to a pounding effect of the framing members.

**Timber-parapets with strong-backs.** The addition of vertical strong-backs further improved performance of braced parapets, with failure occurring at a peak table acceleration twice the value recorded for timber-braced parapets. The connection of the vertical strong-backs should be designed to transfer the induced base shear loads into the supporting structure.

**Post-tensioned parapets.** Due to insufficient development length below the parapet, the post-tensioning retrofit was unable to prevent out-of-plane failure of the tested parapet and hence further investigation of the appropriate development length is required. Nevertheless, failure occurred at a peak table acceleration six times the value registered for the as-built parapet in the post-cracked condition and 20% lower than for the equivalent steel-braced parapet.

## ACKNOWLEDGEMENTS

The financial support provided by the New Zealand Natural Hazards Research Platform. The valuable efforts of students, researchers, and staff at the University of Auckland are recognised.

## REFERENCES

[1] Giaretton M, Dizhur D, da Porto F, Ingham J. Post-earthquake reconnaissance of unreinforced and retrofitted masonry parapets. Earthq Spectra 2016.

[2] Filiatrault A, Uang C-M, Folz B, Chrstopoulos C, Gatto K. Reconnaissance Report of the February 28, 2001 Nisqually (Seattle-Olympia) earthquake. Report SSRP–2001/02, University of California, San Diego: 2001.

[3] The Masonry Society. Performance of masonry structures in the Northridge, California earthquake of January 17, 1994. A Report by the Investigating Disasters Reconnaissance Team. Austin, Texas: 1994.

[4] FEMA 547. Techniques for the seismic rehabilitation of existing buildings. Prepared by R&C Consulting Engineers and NIST. Federal Emergency Management Agency (USA): 2006.

[5] prEN 1998-1:2003 (E). Eurocode 8: Design of structures for earthquake resistance. Part 1: General rules, seismic actions and rules for buildings. European Standard. European Committee for Standardization (CEN): 2003.

[6] NZSEE. Assessment and improvement of the structural performance of buildings in Earthquakes - Section 10 Revision. Seismic Assessment of Unreinforced Masonry Buildings. New Zealand: New Zealand Society for Earthquake Engineering; 2015.

[7] FEMA P-58/BD-3.9.8. Fragility of masonry parapets. ATC-43 Project - Federal Emergency Management Agency (USA): 2010.

[8] Davey RA, Blaikie EL. Predicted and observed performance of masonry parapets in the 2007 Gisborne earthquake. New Zeal. Soc. Earthq. Eng. Conf. - NZSEE, (Wellington, Mar 26th-28th) New Zealand: 2010.

[9] Lam NTK, Wilson JL, Hutchinson GL. The seismic resistance of unreinforced masonry cantilever walls in low

seismicity areas. Bull New Zeal Soc Earthq Eng 1995;28:179–95.

[10] Griffith MC, Magenes G, Melis G, Picchi L. Evaluation of out-of-plane stability of unreinforced masonry walls subjected to seismic excitation. J Earthq Eng 2003;7:141–69. doi:10.1080/13632460309350476.

[11] Derakhshan H, Dizhur D, Griffith M, Ingham J. Seismic assessment of out-of-plane loaded unreinforced masonry walls in multi-storey buildings. Bull New Zeal Soc Earthq Eng 2014;47:119–38.

[12] NZSEE. Assessment and improvement of the structural performance of buildings in Earthquakes. New Zealand: New Zealand Society for Earthquake Engineering; 2006.

[13] Aleman J, Mosqueda G, Whittaker A. Out-of-plane seismic performance of URM walls with retrofitted parapets and flexible diaphragms. 2nd Conf. Improv. Seism. Perform. Exist. Build. other Struct. - ATC SEI, (San Francisco, December 10th-12th) USA: 2015, p. 328–39.

[14] Bradley BA, Quigley MC, Van Dissen RJ, Litchfield NJ. Ground motion and seismic source aspects of the Canterbury earthquake sequence. Earthq Spectra 2014;30:1–15. doi:10.1193/030113eqs060m.

[15] NZS 1170.5. Structural Design Actions. Part 5: Earthquake actions - New Zealand. New Zealand: 2004.

[16] Almesfer N, Dizhur D, Lumantarna R, Ingham J. Material properties of existing unreinforced clay brick masonry buildings in New Zealand. Bull New Zeal Soc Earthq Eng 2014;47:75–96.